A METHOD TO ANALYSE SCATTERED WAVES FROM BURNT COAL SEAM AND ITS APPLICATION TO ESTIMATE BURNT COAL SEAM THICKNESS IN CENTRAL BORNEO USING A JERS-1 SAR DATA

J. TETUKO S.S. [†,¶], R. TATEISHI[¶], and N. TAKEUCHI[¶]

¶ Centre for Environmental Remote Sensing, Chiba University, 1-33, Yayoi, Inage, Chiba 263-8522, Japan. Phone: +81-43-290-3965, Fax: +81-43-290-3857, Email: tetuko@ceres.cr.chiba-u.ac.jp

† Director of Pandhito Panji Foundation - Research Centre, Jalan Ligar Raya 52B, Bukit Ligar, Bandung 40191, Indonesia. Phone/fax: +62(0)22-2508059, Email: tetuko@ieee.org

KEYWORDS: burnt coal seam, JERS-1, SAR, forest fire, Borneo

ABSTRACT. The interaction of microwaves with rough burnt coal seam is analysed. Analysis medium is composed by three media; i.e. free space (air), burnt coal seam, and perfectly conductor. Polarised and depolarised scattered fields were derived in order to calculate the relationship between burnt coal seam thickness and backscattering coefficient. The result was confirmed by comparing it with results of previous developed method. The result shows different between proposed and previous results. It suspects to be influenced by the roughness of burnt coal seam surface. This relationship was used to estimate burnt coal seam thickness in central Borneo using Japanese Earth Resources Satellite (JERS-1) SAR data. Estimation results and ground data were similar. It shows that the fires penetrated 0.33m under peatland.

1. INTRODUCTION

A simple analysis to solve scattering waves from burnt coal seam using transmission line method was developed (Tetuko et al. 2001), where the roughness of targeted surface was ignored. This paper discusses more complicated scattered wave analysis from rough burnt coal seam. Figure 1 shows distribution of coal seam thickness in the study area: one million hectares peatland project district A (PLG-A) at central Borneo, Indonesia. Ground data was collected from 1995 to 1997 (figure 2). Ground data shows that coal seam surface in the study area has standard deviation d of heights is 1.5m. It means d is larger than wavelength of Japanese Earth Resources Satellite (JERS-1) synthetic aperture radar (SAR) operating frequency (1.275 GHz). Thus, in this research, additional simplifying assumption using the stationary-phase approximation is needed to obtain analytical solutions (Ulaby et al. 1986). In section 2, the analysis of scattered waves from rough burnt coal seam will be discussed. The confirmation of the analysis results by comparing its with results of previous simple analysis is discussed in section 3. Section 4 shows the application of the proposed analysis results to monitor thickness of burnt coal seam in the study area using JERS-1 SAR data. Finally, conclusions are shown in section 5.

2. ANALYSIS

The Kirchhoff or Physical Optics formulation is applicable to surfaces with gentle undulations where average horizontal dimension is large compared with the incident wave (Ulaby et al. 1989). The vector formulation of the Kirchhoff method is based upon the vector second Green's theorem, which states that the scattered field at any point within a source-free region bounded by a closed surface can be expressed in terms of the tangential fields on the surface (Fung et al. 1992). Figure 3 shows geometry of the analysis, the mathematical statement of this fact formulated by Stratton and Chu (Stratton 1941) and modified for the far zone scattered fields is obtained by Silver (Silver 1947). Hence the scattered field in medium 1 (air) is shown as

$$ {}^{o}\boldsymbol{E}^{s} = K_o \hat{\boldsymbol{n}}_{so} \times \int \left[\hat{\boldsymbol{n}}_1 \times \boldsymbol{E} - h_1 \hat{\boldsymbol{n}}_{so} \times \left(\hat{\boldsymbol{n}}_1 \times \boldsymbol{H} \right) \right] \exp\left[jk_1 \left(\hat{\boldsymbol{n}}_{so} - \hat{\boldsymbol{n}}_i \right) \cdot \boldsymbol{r}' \right] d\boldsymbol{S}' \tag{1} $$

where $K_o = -jk_1 \exp(-jk_1 R)/(4pR)$ and R is range from the centre of the illuminated area to the point of observation. $\hat{\boldsymbol{n}}_x$ is unit vector. The approximation relations are obtained from the phase of (1), and by solving the approximated equation, the scattered and depolarised fields are given respectively by

$$ {}^{o}E^{s}_{hh} = M_1 \left(R_{\parallel} \left(\hat{\boldsymbol{h}}_{so} \cdot \hat{\boldsymbol{n}}_i \right)\left(\hat{\boldsymbol{h}}_{\boldsymbol{o}} \cdot \hat{\boldsymbol{n}}_{so} \right) + R_{\perp} \left(\hat{\boldsymbol{v}}_{so} \cdot \hat{\boldsymbol{n}}_i \right)\left(\hat{\boldsymbol{v}}_{\boldsymbol{o}} \cdot \hat{\boldsymbol{n}}_{so} \right) \right) \tag{2} $$

$$ {}^{o}E^{s}_{hv} = M_1 \left(R_{\parallel} \left(\hat{\boldsymbol{v}}_{so} \cdot \hat{\boldsymbol{n}}_i \right)\left(\hat{\boldsymbol{h}}_{\boldsymbol{o}} \cdot \hat{\boldsymbol{n}}_{so} \right) - R_{\perp} \left(\hat{\boldsymbol{h}}_{so} \cdot \hat{\boldsymbol{n}}_i \right)\left(\hat{\boldsymbol{v}}_{\boldsymbol{o}} \cdot \hat{\boldsymbol{n}}_{so} \right) \right) \tag{3} $$

$$ {}^{o}E^{s}_{vv} = M_1 \left(R_{\parallel} \left(\hat{\boldsymbol{v}}_{so} \cdot \hat{\boldsymbol{n}}_i \right)\left(\hat{\boldsymbol{v}}_{\boldsymbol{o}} \cdot \hat{\boldsymbol{n}}_{so} \right) + R_{\perp} \left(\hat{\boldsymbol{h}}_{so} \cdot \hat{\boldsymbol{n}}_i \right)\left(\hat{\boldsymbol{h}}_{\boldsymbol{o}} \cdot \hat{\boldsymbol{n}}_{so} \right) \right) \tag{4} $$

$$ {}^{o}E^{s}_{hv} = M_1 \left(R_{\parallel} \left(\hat{\boldsymbol{h}}_{so} \cdot \hat{\boldsymbol{n}}_i \right)\left(\hat{\boldsymbol{v}}_{\boldsymbol{o}} \cdot \hat{\boldsymbol{n}}_{so} \right) - R_{\perp} \left(\hat{\boldsymbol{v}}_{so} \cdot \hat{\boldsymbol{n}}_i \right)\left(\hat{\boldsymbol{h}}_{\boldsymbol{o}} \cdot \hat{\boldsymbol{n}}_{so} \right) \right) \tag{5} $$

where $M_1 = K_o I_1 E_o q|q_z| \Big/ \left\{\left[(\hat{\boldsymbol{n}}_1 \cdot \hat{\boldsymbol{h}}_{so})^2 + (\hat{\boldsymbol{n}}_i \cdot \hat{\boldsymbol{v}}_{so})^2\right] k_1 q_z\right\}$. $\hat{\boldsymbol{v}}_x$ with $\hat{\boldsymbol{h}}_x$ are unit vector for vertical and horizontal

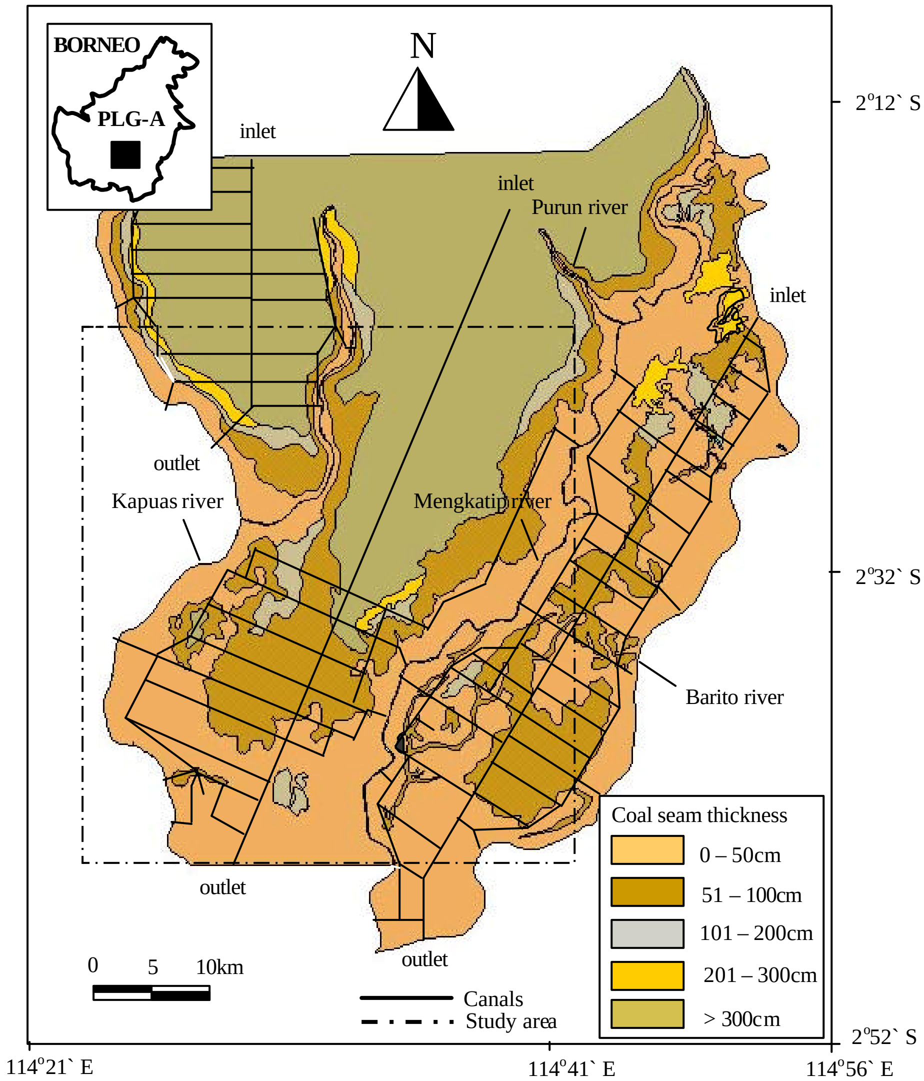

Figure 1. The study area: One Million Hectares Peatland Project (PLG-A) at central Borneo, Indonesia

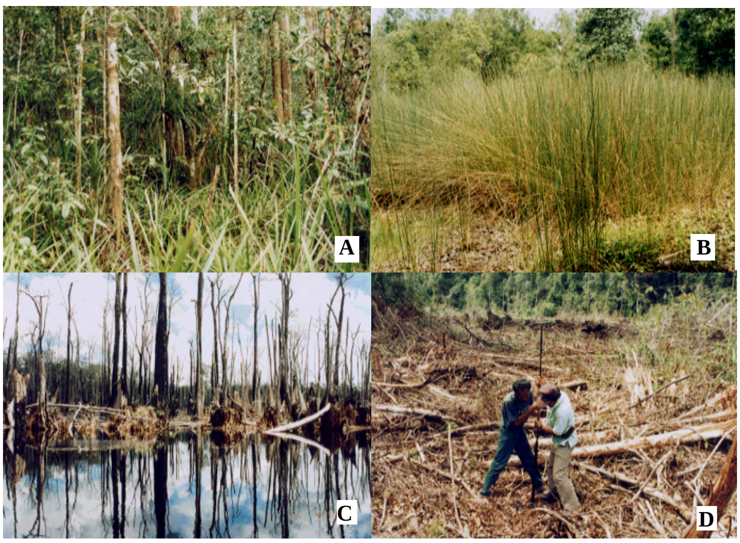

Figure 2. Photographs of field survey expeditions 1995-1997. A and B show main vegetation; tengkawang (*Dipterocarpus spp*), *pule* tree and *purun* grass, respectively. C- burnt forest and coal seam. D- staff measuring thickness of coal seam.

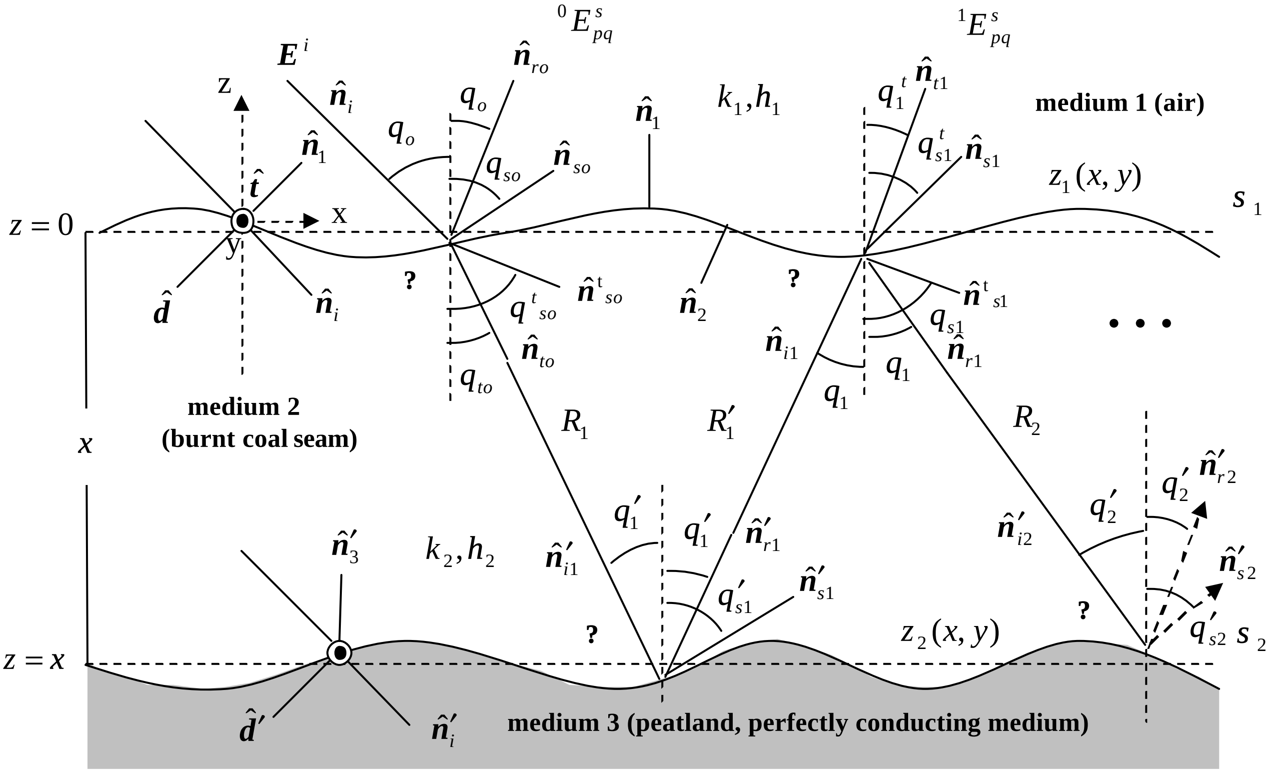

Figure 3. Geometry of the scattering problem.

polarization respectively. R_x is reflectivity. In the similar way to scattered fields in the medium 1, the scattered fields in medium 2 will be obtained as follows

$$ {}^{o}E^{s}_{hh} = -M_2\left(T_\perp(\hat{\boldsymbol{v}}^t_{so}\cdot\hat{\boldsymbol{n}}_i)(\hat{\boldsymbol{v}}_o\cdot\hat{\boldsymbol{n}}^t_{so}) + T_\parallel(\hat{\boldsymbol{h}}^t_{so}\cdot\hat{\boldsymbol{n}}_i)(\hat{\boldsymbol{h}}_o\cdot\hat{\boldsymbol{n}}^t_{so})h_2/h_1\right) \tag{6} $$

$$ {}^{o}E^{s}_{vh} = M_2\left(T_\perp(\hat{\boldsymbol{h}}^t_{so}\cdot\hat{\boldsymbol{n}}_i)(\hat{\boldsymbol{v}}_o\cdot\hat{\boldsymbol{n}}^t_{so}) - T_\parallel(\hat{\boldsymbol{v}}^t_{so}\cdot\hat{\boldsymbol{n}}_i)(\hat{\boldsymbol{h}}_o\cdot\hat{\boldsymbol{n}}^t_{so})h_2/h_1\right) \tag{7} $$

$$ {}^{o}E^{s}_{vv} = -M_2\left(T_\perp(\hat{\boldsymbol{h}}^t_{so}\cdot\hat{\boldsymbol{n}}_i)(\hat{\boldsymbol{h}}_o\cdot\hat{\boldsymbol{n}}^t_{so}) + T_\parallel(\hat{\boldsymbol{v}}^t_{so}\cdot\hat{\boldsymbol{n}}_i)(\hat{\boldsymbol{v}}_o\cdot\hat{\boldsymbol{n}}^t_{so})h_2/h_1\right) \tag{8} $$

$$ {}^{o}E^{s}_{hv} = M_2\left(T_\perp(\hat{\boldsymbol{v}}^t_{so}\cdot\hat{\boldsymbol{n}}_i)(\hat{\boldsymbol{h}}_o\cdot\hat{\boldsymbol{n}}^t_{so}) - T_\parallel(\hat{\boldsymbol{h}}^t_{so}\cdot\hat{\boldsymbol{n}}_i)(\hat{\boldsymbol{v}}_o\cdot\hat{\boldsymbol{n}}^t_{so})h_2/h_1\right) \tag{9} $$

Where T_x is transmittivity. To solving the problem of scattering from a perfectly conducting random surface (②, ④, ⑥,…), the determination of the surface current is considered by a simple surface current estimate $\boldsymbol{J}(\boldsymbol{r}) = \hat{\boldsymbol{n}}'_3 \times \boldsymbol{H}^i$ (Gotoh et al. 1993). The scattered fields for horizontal and vertical polarization and cross polarization are obtained as

$$ {}^{m}E^{s}_{hh} = CE^{m-1}_{hp}\sec q'_m \int dxdy \exp(-2jk_z z) \tag{10} $$

$$ {}^{m}E^{s}_{vv} = CE^{m-1}_{vp}\sec q'_m \int dxdy \exp(-2jk_z z) \tag{11} $$

$$ {}^{m}E^{s}_{hv} = {}^{m}E^{s}_{vh} = 0 \qquad (m = 2, 4, 6, \cdots) \tag{12} $$

where $C = (jk_2/4pR'_m)\exp(-jkR'_m)$ and E^m_{hp} is the field amplitudes at surface of medium 3 that are derived from the scattered fields in medium 2. Then the scattered fields in medium 2 (③, ⑤, ⑦, …) are obtained

$$ {}^{m}E^{s}_{hh} = M_m\left(R_\parallel(\hat{\boldsymbol{h}}_{sm}\cdot\hat{\boldsymbol{n}}_{im})(\hat{\boldsymbol{h}}_m\cdot\hat{\boldsymbol{n}}_{sm}) + R_\perp(\hat{\boldsymbol{v}}_{sm}\cdot\hat{\boldsymbol{n}}_{im})(\hat{\boldsymbol{v}}_m\cdot\hat{\boldsymbol{n}}_{sm})\right) \tag{13} $$

$$ {}^{m}E^{s}_{vh} = M_m\left(R_\parallel(\hat{\boldsymbol{v}}_{sm}\cdot\hat{\boldsymbol{n}}_{im})(\hat{\boldsymbol{h}}_m\cdot\hat{\boldsymbol{n}}_{sm}) - R_\perp(\hat{\boldsymbol{h}}_{sm}\cdot\hat{\boldsymbol{n}}_{im})(\hat{\boldsymbol{v}}_m\cdot\hat{\boldsymbol{n}}_{sm})\right) \tag{14} $$

$$ {}^{m}E^{s}_{vv} = M_m\left(R_\parallel(\hat{\boldsymbol{v}}_{sm}\cdot\hat{\boldsymbol{n}}_{im})(\hat{\boldsymbol{v}}_m\cdot\hat{\boldsymbol{n}}_{sm}) + R_\perp(\hat{\boldsymbol{h}}_{sm}\cdot\hat{\boldsymbol{n}}_{im})(\hat{\boldsymbol{h}}_m\cdot\hat{\boldsymbol{n}}_{sm})\right) \tag{15} $$

$$ {}^{m}E^{s}_{hv} = M_m\left(R_{\|}\left(\hat{\boldsymbol{h}}_{sm}\cdot\hat{\boldsymbol{n}}_{im}\right)\left(\hat{\boldsymbol{v}}_{m}\cdot\hat{\boldsymbol{n}}_{sm}\right) - R_{\perp}\left(\hat{\boldsymbol{v}}_{sm}\cdot\hat{\boldsymbol{n}}_{im}\right)\left(\hat{\boldsymbol{h}}_{m}\cdot\hat{\boldsymbol{n}}_{sm}\right)\right) \tag{16} $$

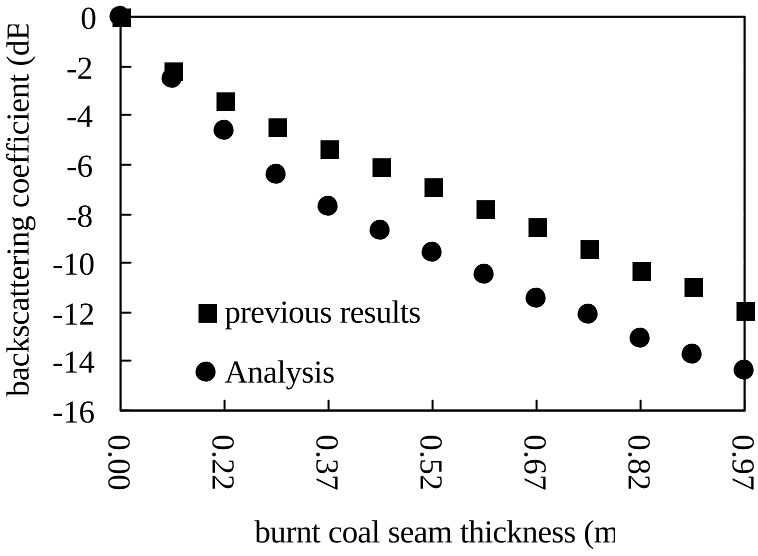

Figure 4. The relationship between burnt coal seam thickness and backscattering coefficient

Where $m = 3, 5, 7, \cdots$, $M_m = K'_m\, I_m E^{s}_{pq}\bar{\bar{q}}_m\left|\bar{\bar{q}}_m\right| \Big/ \left(\left(\left(\hat{\boldsymbol{n}}_2\cdot\hat{\boldsymbol{h}}_{sm}\right)^2 + \left(\hat{\boldsymbol{n}}_{im}\cdot\hat{\boldsymbol{v}}_{sm}\right)^2\right)k_2\bar{\bar{q}}_z\right)$. In the same way, the scattered fields in medium 1 (③, ⑤, ⑦, …) are obtained

$$ {}^{m}E^{s}_{hh} = -M_m\left(T_{\perp}\left(\hat{\boldsymbol{v}}^{t}_{sm}\cdot\hat{\boldsymbol{n}}_{im}\right)\left(\hat{\boldsymbol{v}}_{m}\cdot\hat{\boldsymbol{n}}^{t}_{sm}\right) + T_{\|}\left(\hat{\boldsymbol{h}}^{t}_{sm}\cdot\hat{\boldsymbol{n}}_{im}\right)\left(\hat{\boldsymbol{h}}_{m}\cdot\hat{\boldsymbol{n}}^{t}_{sm}\right)h_1/h_2\right) \tag{17} $$

$$ {}^{m}E^{s}_{vh} = M_m\left(T_{\perp}\left(\hat{\boldsymbol{h}}^{t}_{sm}\cdot\hat{\boldsymbol{n}}_{im}\right)\left(\hat{\boldsymbol{v}}_{m}\cdot\hat{\boldsymbol{n}}^{t}_{sm}\right) - T_{\|}\left(\hat{\boldsymbol{v}}^{t}_{sm}\cdot\hat{\boldsymbol{n}}_{im}\right)\left(\hat{\boldsymbol{h}}_{m}\cdot\hat{\boldsymbol{n}}^{t}_{sm}\right)h_1/h_2\right) \tag{18} $$

$$ {}^{m}E^{s}_{vv} = -M_m\left(T_{\perp}\left(\hat{\boldsymbol{h}}^{t}_{sm}\cdot\hat{\boldsymbol{n}}_{im}\right)\left(\hat{\boldsymbol{h}}_{m}\cdot\hat{\boldsymbol{n}}^{t}_{sm}\right) + T_{\|}\left(\hat{\boldsymbol{v}}^{t}_{sm}\cdot\hat{\boldsymbol{n}}_{im}\right)\left(\hat{\boldsymbol{v}}_{m}\cdot\hat{\boldsymbol{n}}^{t}_{sm}\right)h_1/h_2\right) \tag{19} $$

$$ {}^{m}E^{s}_{hv} = M_m\left(T_{\perp}\left(\hat{\boldsymbol{v}}^{t}_{sm}\cdot\hat{\boldsymbol{n}}_{im}\right)\left(\hat{\boldsymbol{h}}_{m}\cdot\hat{\boldsymbol{n}}^{t}_{sm}\right) - T_{\|}\left(\hat{\boldsymbol{h}}^{t}_{sm}\cdot\hat{\boldsymbol{n}}_{im}\right)\left(\hat{\boldsymbol{v}}_{m}\cdot\hat{\boldsymbol{n}}^{t}_{sm}\right)h_1/h_2\right) \tag{20} $$

Finally, the total scattered field is defined by

$$ E^{s}_{pq} = {}^{0}E^{s}_{pq} + {}^{1}E^{s}_{pq} + {}^{2}E^{s}_{pq} + \cdots = \sum_{m=0}^{\infty} {}^{m}E^{s}_{pq} \tag{21} $$

Mathematically, the total scattering coefficient in medium 1 can be written as

$$ s^{o}_{pq} = 4pR^{2}\,\mathrm{Re}\left\{\left\langle\left|E^{s}_{pq}\right|^{2}\right\rangle\right\} \Big/ A_o\,\mathrm{Re}\left\{\left|E_o\right|^{2}\right\} \tag{22} $$

3. RESULTS

Here backscattering coefficient for scattered field with horizontal-horizontal (HH) polarisation and frequency (1.275 GHz) was calculated. Because the result will be applied to measure burnt coal seam thickness of forest fire scars at central Borneo using JERS-1 SAR data. By substituting each component to each equation of analysis, the correlation between backscattering coefficient and burnt coal seam thickness is obtained as illustrated in figure 4. This figure shows that increment in the thickness of burnt coal seam was directly proportional to reduction in backscattering coefficient. It means that the burnt coal seam absorbed wave energy. Additionally, result of the proposed method is different with the previous results about –2dB. It is suspected occurring by the influenced of roughness in calculation of the analysis. In the next section, the results are applied to estimate the thickness of burnt coal seam in the study area

4. APPLICATION

4.1 Study area

Study area is located 114°23′–114°45′E, 2°23′–2°47′S or at district of south Barito and Kapuas, central Borneo, Indonesia. The altitude of this area is ranging from 9m to 14m above sea level. The Barito river and the Kapuas river encircles this area, and vegetation type of this area is tropical forest. This area is mainly covered by peatland

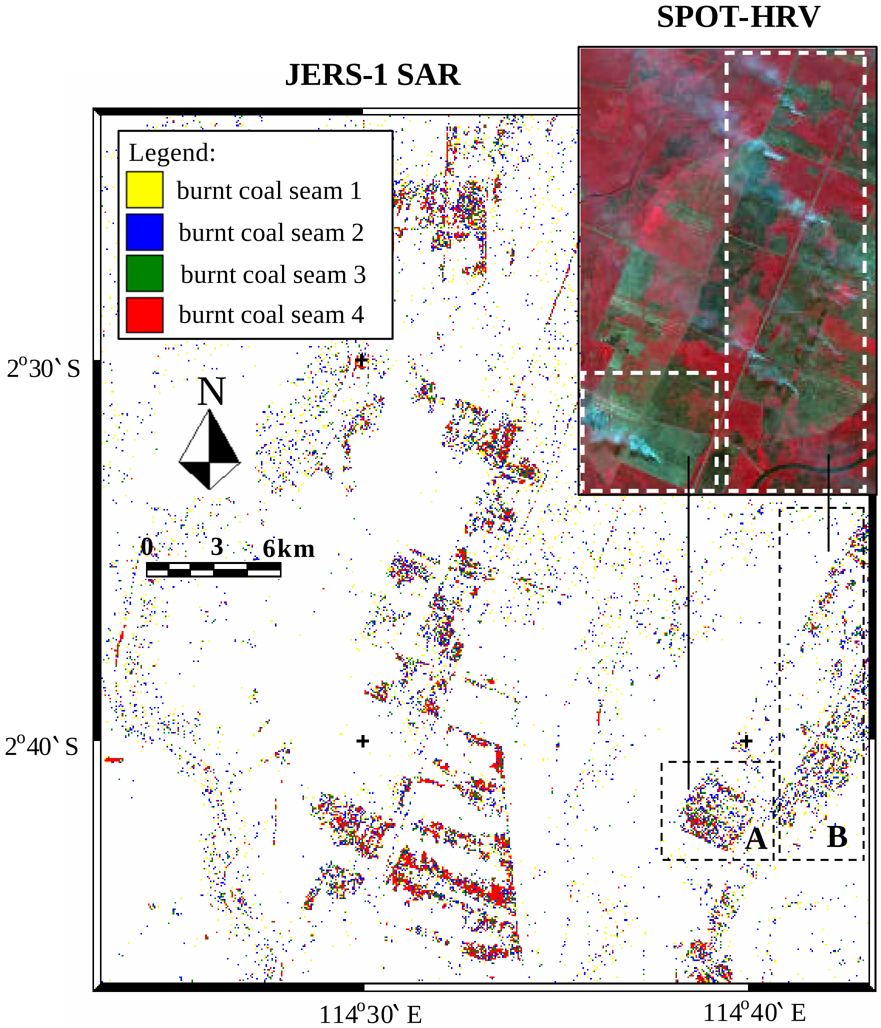

Figure 5. A SPOT-HRV data and supervised classification results of JERS-1 SAR data (29 July 1997).

Table 1. Burnt coal seam thickness in the study area

classes	backscattering coefficient s^{o} [dB]	burnt coal seam thickness ξ [m]
burnt coal seam 1	-7.0	0.23
burnt coal seam 2	-6.5	0.27
burnt coal seam 3	-5.8	0.29
burnt coal seam 4	-5.0	0.33

and peat swamp. The climate on Borneo is wet all through the year with an average annual rainfall of around 3500mm to 4500mm, while the relative humidity varies between 70% and 90%. Ground survey was collected during the period 1995 to 1997 in 'one million hectare peatland project'. The measurement results were mapped (CSAR 1997) (figure 1).

4.2 Data processing

JERS-1 SAR image (path 95, row 305) that was acquired on 29 July 1997 (dry season and during fire events) was used to estimate the thickness of forest fire scars (burnt coal seam) in the study area. This image was processed at level 2.1 or standard geocoded image and was modified into Universal Transverse Mercator (UTM) projection by the Earth Observation Research Centre (EORC) of Japan National Space Development Agency (NASDA). First, a 3x3 median filter was employed and the second process used a 5x5 average filter to reduce inherent speckle noise (Sunar et al 1998). At the same time, the image was also referenced to the UTM co-ordinate system, through a polynomial rectification using 30 ground control points collected from aerial (Bakosurtanal 1990) and topographic maps (Bakosurtanal 1991) of scale 1:50 000. This procedure yielded a geometric accuracy of 0.1pixels. Then the spatial resolution of SAR image was resampled to 12.5m.

A supervised classification was performed to classify the image. The study area was classified into six classes based on aerial and topographic maps and ground data as reference to collect six classes of the training sets. The classes were paddy field, bush swamp, forest, bush land, burnt coal seam, and settlement. The statistic value (average) of each class was obtained and the backscattering coefficient were calculated using the equation $s^{o} = 20\log I - 68.2$ dB (NASDA calibrated equation) (Shimada 1998). Where I is pixel intensity of JERS-1 SAR data. By comparing the results with graph (JERS-1 SAR) in figure 4, burnt coal seam thickness of each class was acquired (table 1) that it was between 0.23m and 0.33m. This result was confirmed by field survey data (figure 1), where area A and B in figure 5 had coal seam thickness of 0~0.50m and 0.51~1m, respectively. It can be said that the analysis results matched well with field survey data.

5. CONCLUSIONS

Numerical analysis was conducted to analyse the relationship between the backscattering coefficients and burnt coal seam thickness ξ. This analysis result was confirmed by comparing it with result of previous developed method. It was about –2dB different result, because influence of the surface roughness. This result was applied successfully in estimating the burnt coal seam thickness in central Borneo, Indonesia. SPOT HRV images were used to ascertain the fire spots in the study area.

This result was confirmed by the ground data that was collected by ground survey done in 1995 to 1997, and it shows that fires could reach 0.33 m deep. This was in good agreement with ground data. Further, application of this result can be used to estimate fire scars thickness, which is very important to extinguish forest fire effectively and accurately.

ACKNOWLEGEMENTS

The authors thank Prof. Koichi Ito, Ichiro Ida, and Kazuyuki Saito for their assistance in measurement of dielectric constants of burnt coal seam samples; MITI/NASDA and CNES for providing JERS-1 SAR and SPOT HRV data, respectively; Franciscus Dwikoco S.S. of Sarana Putra Makmur, Indonesia for ground data, aerial and topographic maps; Nuraini of CSAR, Indonesia for photographs; Satoh International Scholarship Foundation, Atsumi International Scholarship Foundation, and Pandhito Panji Foundation (Innes Indreswari and Pandhito Panji Herdento) for supporting this research.

REFERENCES

BAKOSURTANAL, Aerial photo; Sungai Mantangai 1713-51. Indonesian National Coordination Agency for Surveys and Mapping, 1st edition, BAKOSURTANAL, 1990

BAKOSURTANAL, Topographic maps; Rimbun Tulang 1713-24, Jenamas 1713-52, Dadahup 1713-23. Indonesian National Coordination Agency for Surveys and Mapping, 1st edition, BAKOSURTANAL, 1991.

CSAR, Coal seam thickness map, one million hectares peatland project (PLG-A). Centre for Soil and Agroclimate Research, 1st edition, CSAR, 1997.

Fung, A.K., Li, Z., Chen, K.S., Backscattering from a randomly rough dielectric surface, IEEE Transaction on Geoscience and Remote Sensing, Vol. 30, No. 2, pp. 356- 369, 1992.

Gotoh N., Arai H., Engineering Electromagnetic Waves, p.20, Shokodo, 1993.

Shimada, M., User's guide to NASDA's SAR products. Earth Observation Research Centre (EORC), National Space Development Agency (NASDA), 2nd edition, EORC-NASDA, 1998.

Silver, S., Microwave Antenna Theory and Design, MIT Radiation Lab, Series 12, McGraw-Hill, New York, p.161, 1947.

Stratton, J.A., Electromagnetic Theory, McGraw-Hill, New York, pp.464-469, 1941.

Sunar, F., Taberner, M., Maktav, D., Kaya, S., Musaoglu, N., Yagiz, E., The use of multitemporal radar data in agriculture monitoring: a case study in Kyocegiz-Dalaman ecosystem, Turkey. International Archives of Photogrammetry and Remote Sensing, Vol.32, pp.559-565, 1998.

Tetuko, J.S.S., Tateishi, R., Takeuchi, N., Estimation of burnt coal seam thickness in central Borneo using a JERS-1 SAR image, International Journal of Remote Sensing, 2001 (in press).

Ulaby, F.T., Moore, R.K., Fung, A.K., Microwave Remote Sensing: Active and Passive, Vol. II Radar Remote Sensing and Surface Scattering and Emission Theory, Chapter 12: Introduction to Random Surface Scattering and Emission, pp. 922 – 1033, Artech House, 1986.